ISCI, Volume *20*

Supplemental Information

Longitudinal *In Vivo* Assessment of Host-Microbe Interactions in a Murine Model of Pulmonary Aspergillosis

Shweta Saini, Jennifer Poelmans, Hannelie Korf, James L. Dooley, Sayuan Liang, Bella B. Manshian, Rein Verbeke, Stefaan J. Soenen, Greetje Vande Velde, Ine Lentacker, Katrien Lagrou, Adrian Liston, Conny Gysemans, Stefaan C. De Smedt, and Uwe Himmelreich

Supplementary figures

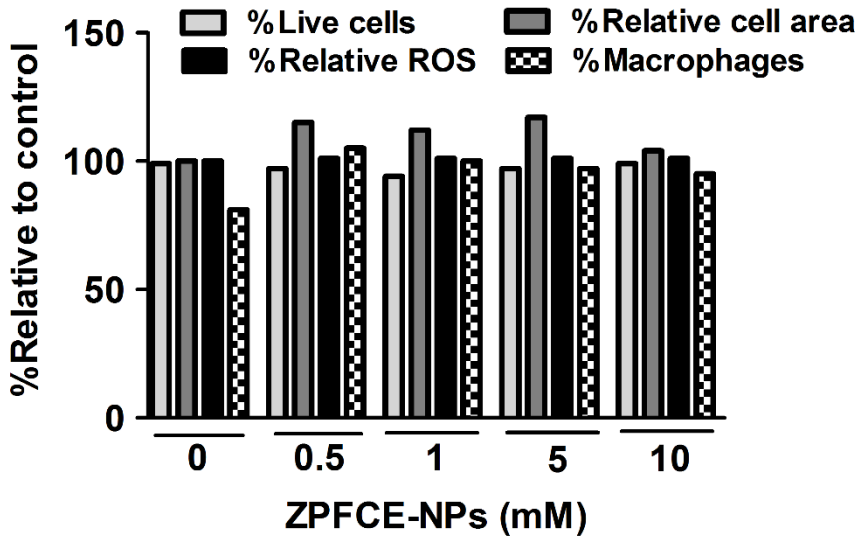

Figure S1. ZPFCE-NP labeling did not show any biological alteration of macrophages, Related to Figures 1 and 2. High-content InCell imaging was performed to evaluate potential cellular toxicity for macrophages upon ZPFCE-NP labeling. Histograms revealed the relative level of cell viability, cell area, formation of mitochondrial reactive oxygen species (ROS) and percentage of macrophages in the total population of immune cells exposed to 0, 0.5, 1, 5, and 10mM of ZPFCE-NPs. Data are represented as mean± SEM of the untreated control values. No statistically significant differences were detected.

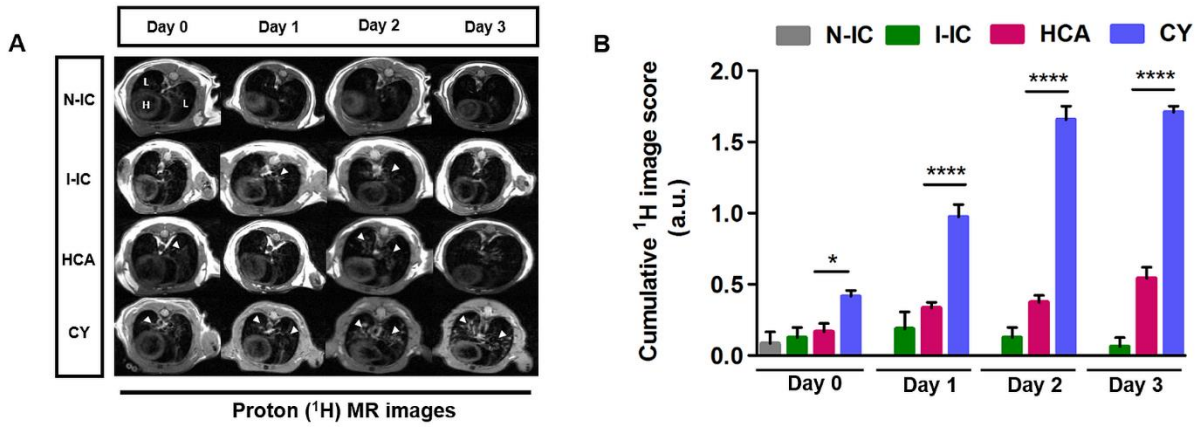

Figure S2. ***In vivo*** **quantification of anatomical changes using ^{1}H MR imaging confirms infection (IPA) and shows lesion development in immunocompromised mice, Related to Figure 3. (A)** ^{1}H MR images were acquired before ^{19}F MRI acquisition using a dual-tuned MR coil. ^{1}H MRI images were acquired daily from the day of infection for three days. Lesions caused by *A. fumigatus* infection are seen as hyperintense (bright) regions (arrow). **(B)** Quantitative estimation of lung lesion development was performed based on the image signal intensities by applying cumulative image scoring method. (N-IC: Non-infected immunocompetent group, *n*=3; I-IC: Infected-immunocompetent group, *n*=4; HCA: Hydrocortisone acetate treated group, *n*=5; CY: Cyclophosphamide treated group, *n*=6). Data represented as mean±SEM. ($*$ $p<0.05$, ****$P<0.0001$).

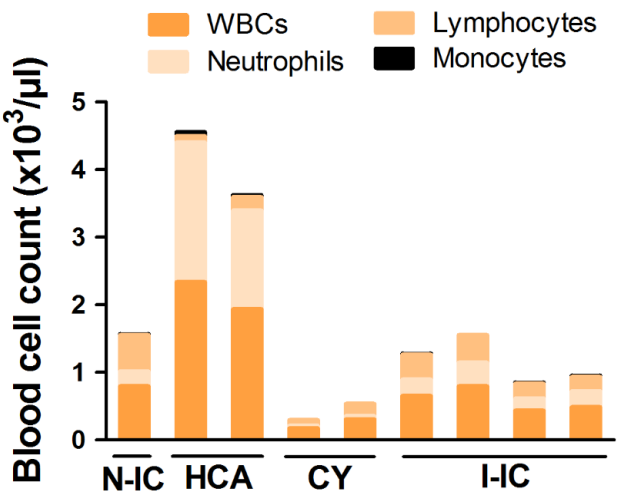

Figure S3. Differential blood immune cell counting depicts patrolling immune cells in all murine groups, Related to Figures 3 and 5. Samples from peripheral blood pool was analyzed for individual mice after cardiac puncturing. Blood samples were collected from different groups on the experimental end-point at day 3. Numbers of white blood cells (WBCs), neutrophils, lymphocytes and monocytes were measured and represented for individual animal.

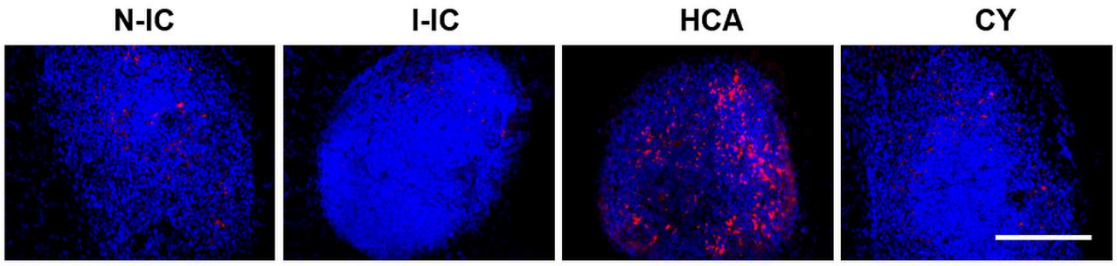

Figure S4. Visualization of ZPFCE-NPs in cervical lymph nodes confirms *in vivo* ^{19}F MRI assessment for all mice groups, Related to Figure 3C. Fluorescent microscopy was performed on cryo-sectioned cervical lymph nodes where high accumulation of ZPFCE-NPs in the lymph nodes was shown in HCA group compared to other groups after animals have been sacrificed on day 3, after infection. Scale bar 100µm. Stainings: Blue=DAPI, Red=ZPFCE-NPs.

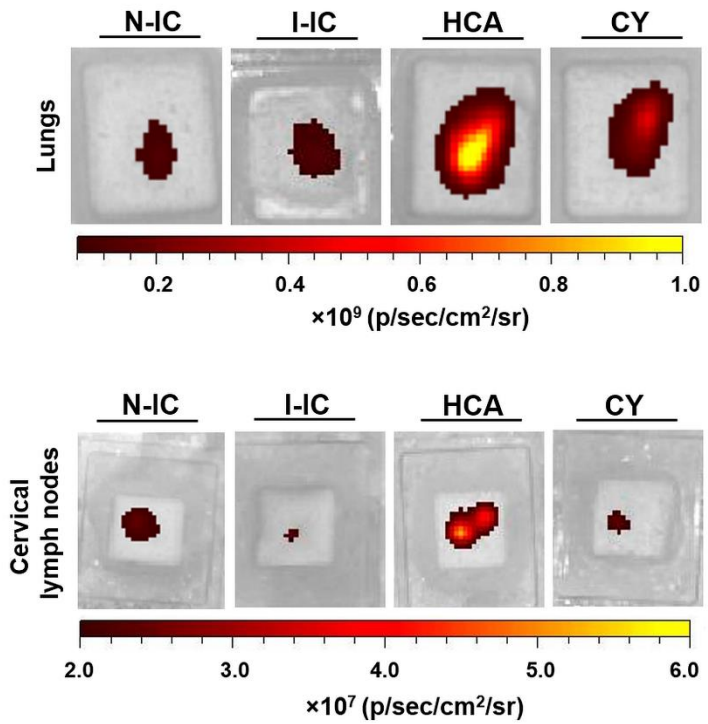

Figure S5. ***Ex vivo*** **fluorescence imaging of lungs and cervical lymph nodes using IVIS Spectrum system confirms ^{19}F MRI, Related to Figures 3 and 4.** Fluorescence images on the cryopreserved OCT-embedded lungs and cervical lymph nodes from all groups of mice were performed after the experimental end-point, three days post-infection. The scale bar represents fluorescence signal intensity. High signal intensities were detected in the lungs and lymph nodes of HCA-treated mice, confirming accumulation of ZPFCE-NP-labeled immune cells.

Transparent method section

Animals

For the *in vitro* labeling experiments, macrophages were isolated from the peritoneum of C57/BL6 female mice (8-9 week-old). Female OT-II mice (6-8-week-old) bearing the MHCII-restricted T cell receptor (TCR) for $OVA_{323–339}$ were bred in house. For *in vivo* experiments, 10-week-old male Balb/c mice (Janvier, Le Genest, France) were housed in KU Leuven animal housing facility with free access to food and water.

All animal experiments were approved by the Ethical Committee of KU Leuven and were conducted according to the Belgian (Royal Decree of 29 May 2013), Flemish (Decision of the Flemish Government to adapt the Royal Decree of 29 May 2013, 17 February 2017) and European (Directive 2010/63/EU) regulations on the protection of animals used for scientific purposes.

Synthesis of fluorinated Zonyl-PFCE nanoparticles

The synthesis of biochemically inert perfluoro-15-crown-5-ether (PFCE) nanoparticles consisting of a PFCE liquid core emulsified by a monolayer of phospholipids was performed as described previously (Dewitte et al., 2013). The fluorosurfactant Zonyl® FSP (Du Pont, Delaware, USA) was incorporated in the lipid shell of PFCE nanoparticles, obtaining nanoparticles with an average size of 280nm. For the *in vitro* and *in vivo* experiments, ZPFCE-NPs were coupled with either Cholestryl BODIPY® FLC12 or DiR fluorescent dye (both from Molecular Probes, Invitrogen, Merelbeke, Belgium).

In vitro labeling of macrophages using ZPFCE nanoparticles

For *in vitro* labeling, cells were incubated with ZPFCE-NPs at fluorine concentration of 0.5, 1 and 10mM for 1h at 37°C in 5% CO2 in ultra-low attachment plates (Corning Costar, Kennebunk, ME, USA). For positive selection of labeled macrophages, cells were analyzed for surface marker expression after pre-incubation with the Fc receptor blocking antibody anti-CD16/CD32 (eBioscience, San Diego, CA, USA) and staining using anti-F4/80 and anti-CD11/b (eBioscience, San Diego, CA, USA) to perform quantitative flow cytometric analyses.

Toxicological assay on ZPFCE-NP labeled macrophages

Primary macrophages were labeled with different concentrations of ZPFCE-NPs. Surface staining with anti-F4/80 (eBiosciences) was performed to identify macrophages by microscopic analysis. Following exposure to nanoparticles, immune cells were stained to assess cell viability, cytoskeletal changes and oxidative stress. Data analysis was performed using a high-content InCell 2000 analyzer (GE Healthcare Life Sciences, Diegem, Belgium) as previously described (Manshian et al., 2014)**.**

Determination of cytokine secretion by ZPFCE-NP labeled macrophages

For cytokine measurement, ZPFCE-NP labeled macrophages were co-cultured in the presence or absence of 1µg/mL lipopolysaccharides (Sigma Aldrich, Overijse, Belgium) for 24h. Supernatants were collected and measurements of IL-10, IL-1beta and TNF-alpha were performed using a customized MSD V-PLEX mouse proinflammatory kit (Mesoscale, Maryland, USA). Readings were performed using a MESO QuickPlex SQ120 plate reader (Mesoscale, Maryland, USA).

In vitro adaptive immune test on ZPFCE labeled macrophages

Splenocytes from OTII transgenic mice were homogenized and negative selection of purified total CD4+ T cells was performed using a cocktail of antibodies for CD16/CD32, CD11b, CD11c, B220, MHC-II and CD8 markers. Contaminating, bead-bound cells were removed using sheep-anti-rat IgG paramagnetic beads, according to the manufacture's specifications (Dynabeads, Invitrogen Merelbeke, Belgium). Purity of samples (>95%) was routinely assessed by flow cytometry. Purified OTII-transgenic CD4+ T cells were co-incubated with ZPFCE-NP labeled macrophages in a 96 well plate together with variable doses of anti-TCR b5.1/b5.2 (OTII) peptide at concentrations of 0, 0.1, 1, 10μg/ml for 1-3 days at 37°C under 5% CO_2 for 1h. To prevent non-specific binding all surface stains were performed in the presence of anti-CD16/CD32. For macrophages, the antibodies F4/80-PerCPCy5.5, CD45-APC-eFluor780 and CD11b-eFluor450 were used. To stain T cells, CD44-FITC, TCRb5.1/5.2-PE, CD62L-Per CPCy5.5, CD69-PECy7 and CD4-eFluor450 were used to assess effector, memory and naïve CD4+ T cell subsets using flow cytometry. All antibodies were purchased from eBioscience (San Diego, CA, USA).

Murine models of invasive pulmonary aspergillosis

To develop a non-neutropenic IPA model, mice were injected subcutaneously (s.c.) with 9mg hydrocortisone acetate per 25g body weight (Sigma-Aldrich, USP, Overijse, Belgium) one and three days before inoculation with *A. fumigatus* (HCA group, *n*=9). To induce neutropenia, 200mg kg^{-1} body weight cyclophosphamide (Sigma-Aldrich, USP, Overijse, Belgium) was injected intraperitoneally (i.p.) one and three days before inoculation with *A. fumigatus* (CY group, *n*=9). Infected immunocompetent mice (I-IC group, *n*=4) and non-infected immunocompetent mice (N-IC, *n*=3) were included as control groups.

The Fluc^{+} *A. fumigatus* strain 2/7/1 was generously provided by M. Brock (School of Life Sciences, University of Nottingham, UK). The strain was cultured and conidia were harvested using a previously described protocol (Poelmans et al., 2016). On day of infection (day 0), HCA and infected immunocompetent groups (I-IC group, n=4) were intranasally instilled with 1×10^{6} spores. The CY group was inoculated with 5×10^{5} spores based on the protocol described previously (Poelmans et al., 2016). ZPFCE-NPs were administered via tail vein 1h prior to MRI acquisition on day 0 and day 1. On the day of inoculation (day 0), MRI experiments were performed on all mice groups 4h after the administration of spores. All murine groups were monitored for weight loss and posture changes starting from day 0 to detect onset of disease symptoms and to define the humane end-points.

Longitudinal in vivo fluorine (^{19}F) magnetic resonance imaging

Animals were anesthetized by intraperitoneal (i.p.) injections of ketamine (45-60 mg kg^{-1}, Nimatek, Eurovet animal health, Bladel, The Netherlands) and Medetomidine (0.6-0.8 mg kg^{-1}, Domitor, The Orion Pharma, Espoo, Finland) solution. *In vivo* longitudinal follow-up of all murine groups was performed using ^{1}H and ^{19}F MRI on a 9.4T preclinical MRI scanner (Bruker Biospec 94/20, Ettlingen, Germany). After the MR acquisition, injections of atipamezole (Antisedan, The Orion Pharma, Espoo, Finland) were administered i.p. to reverse the effects of anesthesia. Throughout the MR imaging experiments, body temperature and respiration rate of the animals were monitored and maintained to 37°C and 60-80 min^{-1}, respectively.

A purpose-built dual-tuned radio frequency surface coil was used to acquire fluorine and ^{1}H MR images. For all *in vivo* MRI experiments, 2D RARE (Rapid Acquisition with Relaxation Enhancement) MRI was performed using the following acquisition parameters: ^{1}H MRI, repetition time (TR) = 3500ms, echo time (TE) = 6.12ms, spatial resolution = 0.156mm×0.156mm, slice thickness = 1mm. For ^{19}F MRI, TR = 5388ms, TE = 6.11ms, spatial

resolution = 1.25mm×1.25mm, slice thickness = 2mm were used. A reference tube containing 30mM of ZPFCE-NPs embedded in agar was placed next to the abdomen of the animal during the MR acquisition to allow quantification of fluorine atoms. For both ^{1}H and ^{19}F MR images, data were acquired with the same localization (placement, orientation of slice packages).

Quantification of ^{19}F MR signal and data processing

Prior to the MR signal quantification, images were reconstructed using the Paravison 5.1 software (Bruker Biospin, Ettlingen, Germany). For post processing, MR images were exported to the MeVislab software version 2.6.1 (MeVis Medical Solutions AG, Bremen, Germany). Gaussian smoothing was applied to the ^{19}F MR images. Before masking the fluorine images, interval thresholding was performed by applying a value higher than the background noise. Masked ^{19}F MR images were rescaled to the same matrix size as the ^{1}H MR images before superimposing them over each other. To calculate the amount of fluorine atoms/voxel, the processed ^{19}F MR images were analyzed slice-wise using the Fiji software, version 1.49a (South Carolina, USA) by drawing the region of interests on the fluorine hot spots in the lungs and the lymph node regions, which were identified based on the anatomical ^{1}H MR images. For quantification, regions were compared with the reference tube that contained 30mM ZPFCE-NPs. Cumulative ^{1}H image scoring was performed on ^{1}H images of all murine groups from day 0 to day 3. Based on the visual observations, lung lesions were identified and a scoring system was used to assign a value for the quantification of signal intensities corresponding to the disease development as described previously (Petraitiene et al., 2002; Petraitis et al., 2003).

Ex vivo bioluminescence imaging

On day 3, the animals were euthanized and the lungs were inflated with 0.5ml D-luciferin (7.5mg) (Promega, Leiden, The Netherlands) by inserting a 22-gauge catheter (Terumo, Heverlee, Belgium) into the trachea. The lungs were immediately placed into the flow chamber

to perform *ex vivo* BLI acquisitions on the IVIS Spectrum imaging system (Perkin Elmer, Massachusetts, USA). Data were analyzed using Living Image® software version 4.5.5 (Perkin Elmer, Massachusetts, USA).

Differential white blood cell measurements

For the differential blood cell counting, mice were euthanized under deep terminal anesthesia and blood was withdrawn using a 25-gauge needle (Terumo, Heverlee, Belgium) from the left ventricles of the beating heart through cardiac puncturing. Total collected blood volume was 0.3 ml from each mouse. To prevent coagulation of blood, 30µl of tri-sodium citrate, 3.8% w/v (VWR, Belgium) was added to the blood collection tubes. Blood cell counts were performed on an ADVIA®2120i hemocytometer, version 5.4 (Siemens Healthcare, GmbH, Erlangen, Germany).

Colony-forming unit (CFU) measurements

After the *ex vivo* BLI acquisition, the right lung lobes were collected in 600µl PBS and homogenized to obtain suspensions of lung tissue. Lung homogenates were plated on Sabouraud agar, followed by an incubation period of 2-3 days at 30°C for manual counting of CFUs.

Flow cytometry and microscopy

Flow cytometry acquisitions were performed on a Gallios™ flow cytometer (Beckman Coulter, Brea, California, USA). For the data analyses, a FlowJo software, version 10.4.2 (FlowJo LLC, Ashland, Oregon, USA) was used. Microscopic images were acquired using a confocal microscope (Nikon, Tokyo, Japan) and analyzed using Fiji software, version 1.49a (South Carolina, USA).

Ex vivo optical imaging of lungs and cervical lymph nodes

Ex vivo fluorescence imaging was performed on the lungs and cervical lymph nodes (LN) of all animals using the IVIS Spectrum imaging system (Perkin Elmer Massachusetts, USA). For the acquisition of data, parameters used are as following: exposure time = 10sec, 740nm excitation and 800nm emission filters with medium binning. Data analysis was performed using the Living Image® software, version 4.5.5 (Perkin Elmer, Massachusetts, USA).

Histology and immunohistochemistry

Right lung lobes were fixed in 4% PFA and embedded in paraffin. For visualization of fungi, lungs were sectioned (5µm) and stained with Periodic acid-Schiff (PAS) agent as described (Poelmans et al., 2016). Brightfield images were acquired using ZEISS Axio Scan.Z1 Digital Slide Scanner (Carl Zeiss, Oberkochen, Germany). For immunoflurosence, left lung lobes were fresh frozen in OCT (optimum cutting temperature) formulation and cryosections (11µm) were fixed in 4% paraformaldehyde and stained according to manufacturer's protocol. For staining of the sections following monoclonal antibodies were used: GR1 (RB6-8C5, eBioscience), CD11b (M1/70, Biolegend), CD11c biotin (N418, eBioscience). For the staining of immune cells, the following detection antibodies were used: Donkey anti-Rat 488, Streptavidin 546, (all from Molecular Probes). Images were acquired using a EVOS FL Auto 2 microscope (Fisher Scientific, Merelbeke, Belgium).

Statistical analysis

For statistical analyses, One-way and Two-way ANOVA tests were performed together with Bonferroni multiple comparison test to compare the different animal groups using the GraphPad Prism software®, version 5.04 (La Jolla, CA, USA).

Supplemental references

Dewitte, H., Geers, B., Liang, S., Himmelreich, U., Demeester, J., De Smedt, S.C., Lentacker, I., 2013. Design and evaluation of theranostic perfluorocarbon particles for simultaneous antigen-loading and19F-MRI tracking of dendritic cells. J. Control. Release 169, 141–149.

Manshian, B.B., Moyano, D.F., Corthout, N., Munck, S., Himmelreich, U., Rotello, V.M., Soenen, S.J., 2014. High-content imaging and gene expression analysis to study cell-nanomaterial interactions: The effect of surface hydrophobicity. Biomaterials 35, 9941–9950.

Petraitiene, R., Petraitis, V., Groll, A.H., Sein, T., Schaufele, R.L., Francesconi, A., Bacher, J., Avila, N.A., Walsh, T.J., 2002. Antifungal efficacy of caspofungin (MK-0991) in experimental pulmonary aspergillosis in persistently neutropenic rabbits: Pharmacokinetics, drug disposition, and relationship to galactomannan antigenemia. Antimicrob. Agents Chemother. 46, 12–23.

Petraitis, V., Petraitiene, R., Sarafandi, A. a, Kelaher, A.M., Lyman, C. a, Casler, H.E., Sein, T., Groll, A.H., Bacher, J., Avila, N. a, Walsh, T.J., 2003. Combination therapy in treatment of experimental pulmonary aspergillosis: synergistic interaction between an antifungal triazole and an echinocandin. J. Infect. Dis. 187, 1834–1843.

Poelmans, J., Hillen, A., Vanherp, L., Govaerts, K., Maertens, J., Dresselaers, T., Himmelreich, U., Lagrou, K., Vande Velde, G., 2016. Longitudinal, in vivo assessment of invasive pulmonary

aspergillosis in mice by computed tomography and magnetic resonance imaging. Lab. Invest. 96, 692–704.